Aust. J. Phys., 1995, **48**, 953–70

An Overview of Recycling in Laser Interferometric Gravitational Wave Detectors*

David E. McClelland

Department of Physics, Faculty of Science,
Australian National University,
Canberra, ACT 0200, Australia.

email: David.McClelland@anu.edu.au

Abstract

Recycling refers to optical techniques used in laser interferometers to enhance their signal response for a given input power. Driven by the quest to detect gravitational waves using interferometers, a host of configurations have been proposed over the last ten years. Here, these techniques are summarised, and their tolerance to wavefront distortion considered along with their applicability to long and mid baseline laser interferometers.

1. Introduction

The prediction from Einstein's general theory of relativity (Einstein 1915*a–d*, 1916) of the existence of waves of space–time curvature, or gravitational waves, followed by proof that these waves could do work (Pirani 1957; Bondi 1957) and therefore potentially be detectable, led to Weber's (1966, 1987) pioneering experiments in the 1960s. Though ultimately proving to be unsuccessful, Weber's worked inspired researchers world wide to take up the challenge. Initially the best sensitivities were achieved using resonant bar detectors along the Weber line, but cooled to liquid helium temperatures. Today, such instruments have a strain sensitivity (fractional change in length divided by the length) in the 10^{-19} range, over a bandwidth of a few Hertz. One of the most sensitive of these detectors is currently in operation at the University of Western Australia (see Tobar *et al.* 1995; present issue p. 1007). Methods have been proposed to push below this sensitivity; to increase the bandwidth of such instruments; and to build omnidirectional sensors (Hamilton 1995).

The strain sensitivity of current instruments is still a few orders of magnitude off the performance required to detect gravitational waves on a regular basis (a few events per year). In the 1970s research into an alternative technology, laser interferometry, began in earnest. It had been known since the famous Michelson–Morley experiments in 1887 that interferometry is an extremely sensitive method to measure length changes. Following the proposal by Gersenshtein and Pustovoit in 1963, Moss *et al.* (1971) commenced the first serious endeavour in this field. State-of-the-art prototype interferometers in operation at the University of Glasgow and at CALTECH now record sensitivities comparable to that of the

* Refereed paper based on a contribution to the inaugural Australian General Relativity Workshop held at the Australian National University, Canberra, in September 1994.

0004-9506/95/060953$10.00

resonant bar devices (Ward *et al.* 1995; Raab 1995). These instruments have baselines of a few tens of metres. It is therefore predicted that interferometers with baselines of a few kilometres will be capable of detecting a few gravitational wave events per year. It is to this end, that the LIGO Project (Vogt 1991) in the United States and the VIRGO project (Brillet *et al.* 1992) in Europe have begun.

Laser interferometers of the Michelson design with orthogonal arms are ideally suited to detect gravitational waves. In one gauge, it can be viewed that an optimally oriented gravitational wave will alternately stretch then contract one arm whilst contracting then stretching the other arm: the stretching and contracting reversing every half period of the wave, $\tau/2$. In the simplest form of interferometer, the phase difference between light in the orthogonal arms, read out by interference at the main beamsplitter, will be a maximum if the light is stored in the arms for a time on the order of $\tau/2$. Given a typical gravity wave frequency of 500 Hz, this then requires a storage time of a millisecond. This can be achieved over a reasonable baseline, by inserting light storage devices in the arms of the interferometer: either delay lines or Fabry–Perot cavities. In an ideal device free from any noise, many bounce delay lines or ultra-high finesse cavities could be used with no great restriction on the interferometer baseline.

In fact there are many sources of noise affecting the interferometer, some technical and capable ultimately of being overcome, others fundamental. By far the most important source of technical noise is thermal noise (Saulson 1990, 1991) arising from mechanical loss in the interferometer optics and suspension systems. In general, the importance of thermal noise scales inversely with armlength. It is indeed to reduce this type of noise that interferometers with baselines of a few kilometres are being constructed.

Ultimately, it is quantum mechanics which imposes sensitivity restrictions. The Heisenberg Uncertainty Principle must be applied to the position of the masses which form the mirrors. This limitation also scales inversely with length. With a typical mass of 30 kg, this *standard quantum limit* (SQL) is well below thermal noise. A second quantum mechanical restriction arises from application of the uncertainty principle to the light. Caves (1980, 1981) showed that this was manifested in two ways: fluctuations in the number of photons leaving the device, referred to as the photon counting error; and light pressure induced fluctuations on the mirrors (radiation pressure error). There is a trade off between these error sources which leads to an optimum input power, at which the sensitivity limit is equal to the SQL. However, at currently envisaged light powers, radiation pressure error can be ignored. An instrument limited by photon counting error is commonly referred to as being photon or shot noise limited.

In general, shot noise scales inversely with the square root of the laser power in the interferometer. It is therefore important to minimise losses in optical components. The longer the armlength the fewer the number of light reflections in the arm storage device, hence the less total loss. With losses on the order of 1 or 2 ppm, baselines of only a few hundreds of metres could be used.

Curve (i) in Fig. 1 depicts a typical sensitivity, given as a noise spectral density versus frequency plot, for a laser interferometer gravitational wave detector. It is based on parameters for the VIRGO project. It can be broken up into three regions: seismic noise, thermal noise and shot noise. At very low frequencies

seismic noise limits the performance. Techniques developed at the University of Western Australia (Ju and Blair 1994) and in Pisa, Italy (Del Fabbro *et al.* 1988) should render seismic noise negligible above 50 Hz. The second region is thermal noise dominated. Depending on the length of the instrument, the optical arrangement, and the technology used, this region could extend from 50 Hz to anywhere between 100 and 1000 Hz. Above this frequency, shot noise ultimately limits performance. This third region of Fig. 1 is the focus of this paper. It is in such regions that the techniques known collectively as recycling can be applied.

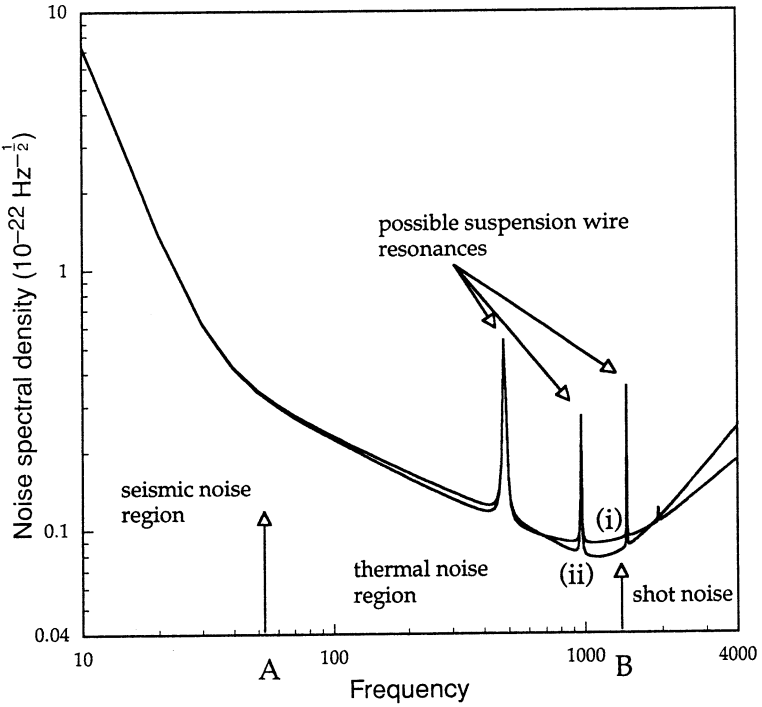

Fig. 1. (i) Typical frequency spectral noise density for laser interferometer gravitational wave detectors (based on VIRGO parameters). The diagram shows three regions: seismic noise is dominant up to frequency A; thermal noise dominates between A and B; shot noise is dominant above B. The resonant peaks arise from violin modes in the suspension wires. (ii) Spectral noise density for the same interferometer, but with dual recycling, tuned to 1 kHz, implemented. The amplitude reflectivity of the signal recycling mirror was set to 0·8.

The first of these techniques, proposed by Drever (1983), is now known as power recycling. In essence the input laser beam, referred to as the carrier, is impedance matched into the interferometer via an input mirror (M0 in Fig. 2). Using this technique, the 'effective' input power, i.e. the light hitting the main beam splitter, can be increased by up to a factor equal to the inverse of the total losses. The (shot-noise-limited) sensitivity is improved by the square root of this factor.

Power recycling is inherently broadband, leaving the bandwidth of the interferometer essentially unaffected. By increasing the total power in the device, power recycling increases the amount of light appearing as signal sidebands. Subsequent recycling techniques, such as resonant (or synchronous) recycling (Drever 1983) and signal recycling (Meers 1988), seek to improve the efficiency of power transfer between carrier and signal. This is achieved by making the interferometer resonant at one of the sideband frequencies. This effectively couples the two arms of the Michelson interferometer. In general this leads to enhancement of signal response at the expense of bandwidth. As explained in Section 3, an important side effect of the coupling is that these instruments are less sensitive to wavefront distortions (Meers and Strain 1991; McClelland *et al.* 1993).

In the next section, the various recycling configurations will be described: power recycling; resonant recycling; detuned recycling; signal recycling; doubly resonant signal recycling; and finally resonant sideband extraction. In Section 3 the merits of various arrangements in terms of tolerance to wavefront distortions are considered. Section 4 addresses the use of recycling in planned instruments. It is worth noting that, at the time of writing, only power recycling and broadband dual recycling have been demonstrated in the laboratory.

2. Recycling Techniques

(2a) Power Recycling

Operating an interferometer at a dark fringe on the output port (see Fig. 2 without mirror M3) minimises shot noise, suppresses technical noise present on the drive laser and maximises signal recovery (see Stevenson *et al.* 1995; present issue p. 971). Now the action of a gravitational wave of frequency ω_g on the instrument results in phase modulation of the light, shifting energy into sidebands at frequencies $\omega_L \pm \omega_g$, where ω_L is the laser frequency. At the main beamsplitter, the signal sidebands are directed to the output photodetector, whilst light in the fundamental mode at the driving laser (carrier) frequency is reflected back toward the laser. A partially reflecting mirror (M0 in Fig. 2) between the laser and the beam splitter reuses this 'waste light' by coherently reflecting it back into the interferometer. Effectively, an optical build up cavity, known as the power recycling cavity (PRC), has been formed.

Fig. 3 plots the frequency response of a power recycling, 3 km long, Michelson interferometer relative to the response of the same instrument with no power recycling. Its response is broadband and increases with the square root of the circulating power, as predicted. Maximum circulating power, and hence maximum sensitivity, is achieved when the laser is impedance matched into the cavity, that is, when the transmission of mirror M0 is equal to the total losses.

The first experimental test of power recycling was performed by Maischberger *et al.* (1988) using a 3 m long single bounce Michelson interferometer. A recycling factor of 9 was achieved. Further experimental tests have been performed on both benchtop and suspended instruments (Man *et al.* 1990; Meers and Strain 1991; Gray 1995; Tsubono 1995), and with benchtop Fabry–Perot arm cavity systems (Fritschel *et al.* 1992; Regehr 1994). To date, the largest recycling factor is of the order of 60.

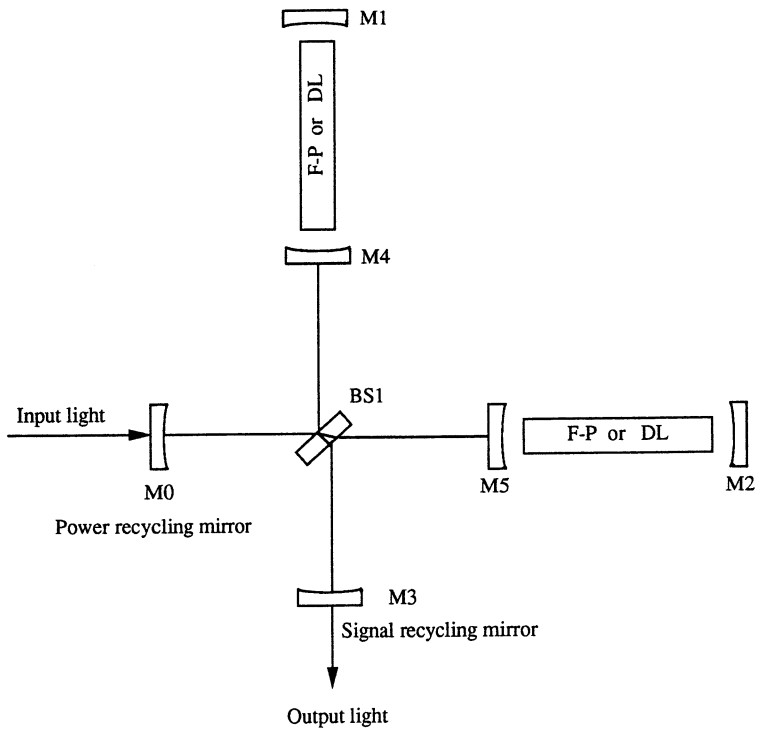

Fig. 2. Optical configuration for power recycling, signal recycling, and resonant sideband extraction (RSE). When only power recycling is employed, mirror M3 is not present. Typical finesse for the arm cavities is 50. For dual recycling, the M3 parameters are adjusted for tuning frequency and bandwidth. The signal is not resonant in the SRC. In the case of RSE, the Fabry–Perot cavities would have very high finesse (3000 or more) for the carrier and M3 parameters are adjusted to extract the signal, after optimum storage time.

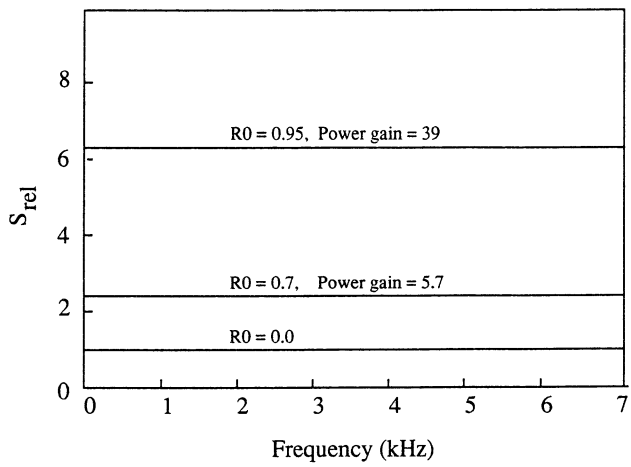

Fig. 3. Frequency response S_{rel} of a single bounce power recycling interferometer, relative to the response of an ideal, single bounce interferometer without recycling. Pump laser power is 10 W. The amplitude reflectivity R0 of the power recycling mirror is 0, 0·7 and 0·95. All mirrors have 1.e-04 intensity loss.

(2b) Resonant Recycling

It was pointed out in Section 1 that light should be stored in an interferometer arm for no longer than half the gravitational wave period. Drever (1983) suggested that by placing a partially reflecting mirror at the position of the beam splitter, as shown in Fig. 4, light leaving the arms after the optimum storage time can be directed into the orthogonal arms where, because the gravitational wave has reversed sign, the induced phase shift would continue to increase. The arms have thus been coupled together forming a cavity with the central partially reflecting mirror as the output coupler. Signal leaks out of the coupler in two directions and is brought to interfere constructively at the beam splitter where it is directed to the photodetection system. Only one signal sideband can be made resonant in this way. By resonantly storing that sideband in the system, light power is more efficiently transferred from the carrier to that sideband. Again light at the carrier frequency is reflected back toward the laser, hence power recycling can also be employed. The maximum gain in sensitivity scales inversely with total optical losses, and is proportional to the ratio of the gravitational wave frequency to the free spectral range (FSR $= c/2L$). At maximum sensitivity, the bandwidth is limited to the FSR times the power losses (Meers 1988).

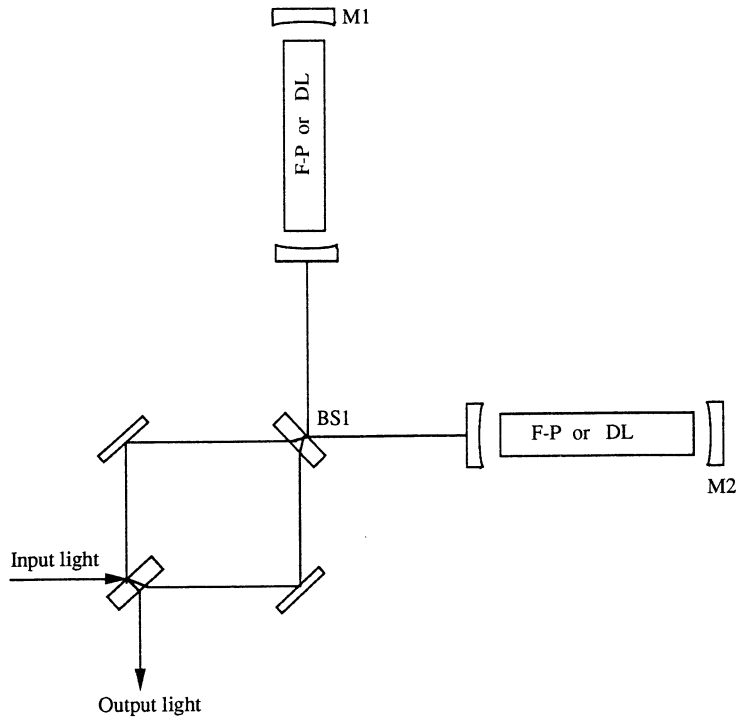

Fig. 4. Optical arrangement for resonant recycling.

When the interferometer contains Fabry–Perot arm cavities, Meers (1988) suggested that it is more informative to consider that the central mirror couples the two cavities. The system then has two normal modes: a symmetric mode in which the carrier light is resonant, and an anti-symmetric mode

in which a signal sideband is resonant. Power is parametrically pumped from the carrier into the signal sideband as the gravitational wave causes the mirror to execute harmonic motion.

(2c) Detuned Recycling

This technique, proposed by Vinet *et al.* (1988), is applicable only when the interferometer has Fabry–Perot cavities in its arms. In the normal mode of operation, the arm cavities are tuned to the carrier. In detuned recycling, these cavities are tuned to a signal sideband, and are therefore highly reflective at the carrier frequency. When coupled to a power recycling cavity, then as with resonant recycling, carrier power can be pumped into signal power. The system exhibits narrowband tuned behaviour with optimum response at the sideband frequency. Sensitivity enhancement and bandwidth restrictions are similar to resonant recycling (Meers 1988).

(2d) Signal Recycling

Signal recycling is another resonant recycling technique. Meers (1988) proposed that the signal could be made resonant by placing a partially reflecting mirror at the output port of the interferometer, shown as mirror M3 in Fig. 2. For simplicity, consider the case of no arm Fabry–Perots. In this layout mirror M3 forms a split optical cavity, known as the signal recycling cavity (SRC), with the end mirrors, M1 and M2. Signal is reflected by M3 back into the interferometer where it adds coherently with more signal being coupled out of the carrier by the action of the gravitational wave. Again signal storage facilitates more efficient transfer of power from the carrier to the sidebands. The combination of signal recycling with power recycling is referred to as dual recycling.

Dual recycling can be operated either in broadband or narrowband mode (Meers 1988). In the broadband case, the SRC is tuned to the carrier frequency. *Provided the signal sidebands lie within the bandwidth of the SRC, they will be enhanced.* In this mode of operation, maximum response occurs at the carrier (zero gravitational wave) frequency.

Operation in the narrowband mode is referred to as tuned dual recycling. In this case, the SRC is tuned to one signal sideband, the other sideband being non-resonant unless it happens to lie at a multiple of a free spectral range. On increasing R3, the response grows around the tuned frequency, and the bandwidth reduces (Fig. 5). Maximum response is achieved when the signal sideband is impedance matched in the SRC; i.e. when transmission of M3 is equal to the total losses. Not surprisingly, the maximum enhancement in response and limiting bandwidth are equivalent to a resonant recycling interferometer.

As the frequency of optimum response is changed by changing the position of mirror M3, signal recycling interferometers can be sensitive to low frequency signals without the need for long arm cavity storage times. The sensitivity/bandwidth combination can be altered by changing the reflectivity of M3. Compound recycling (Section 2*e*) allows this to be simply achieved.

Broadband dual recycling has been experimentally demonstrated using a rigid bench top interferometer (Strain and Meers 1991). An enhancement of the signal-to-noise ratio by a factor of 7 was observed. No other experiments have

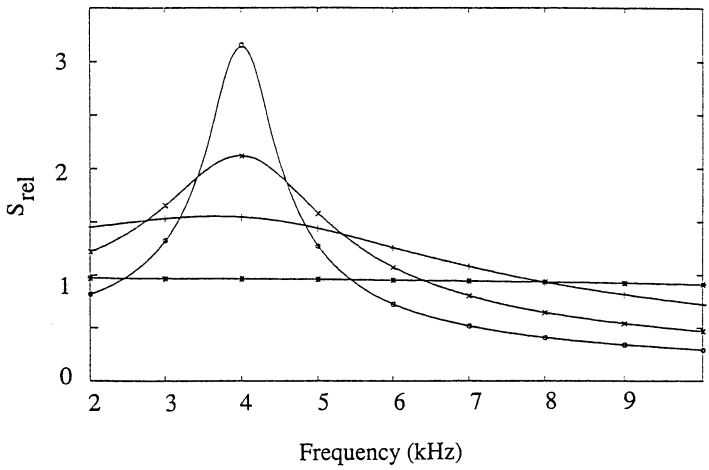

Fig. 5. Frequency response of a tuned dual recycling interferometer relative to a power recycling interferometer, assuming a single bounce delay line in the interferometer arms. Pump laser power is 10 W, the power recycling factor is 39 and the tuning frequency is 4 kHz. The curves, in order of increasing peak response at 4 kHz, are for R3 = 0, 0·7, 0·875 and 0·95. Decreasing the tuning frequency, by moving mirror M3, simply translates these curves toward zero frequency. All mirrors have 1.e-04 intensity loss.

been performed, to date. Benchtop work is in progress at the Australian National University.

(2e) Compound and Doubly Resonant Signal Recycling

Compound recycling is the name coined by Meers and Strain (1991) for an interferometer in which the signal recycling mirror M3 is replaced by a cavity (Fig. 6). The cavity acts as a geometry/frequency dependent mirror. The tuning of this (symmetric) cavity alters its transmission and hence the transmission of the 'compound' mirror and thereby the bandwidth of the detector. In its original form it was suggested that this cavity could be made fairly short with mirrors of very low loss but quite high transmission. Using a short compound mirror (large bandwidth) could overcome the sensitivity bandwidth restrictions inherent in broadband dual recycling.

Later, Meers and Drever (1992) suggested that the compound mirror, when appropriately configured, could enable the SRC to be of high finesse and resonate both signal sidebands without their frequency separation having to correspond to FSRs. This configuration, termed doubly resonant signal recycling, relies on the coupling between the SRC and the compound cavity 'mirror' to split the resonances of the SRC. Meers and Drever showed that by appropriate choice of the mirror transmissions the frequencies of the double resonance can be overlapped with the signal sideband frequencies. The required coupling imposes the constraint of a physically long compound cavity. When losses are negligible, the system will give twice the signal (two sidebands) with half the bandwidth, in comparison with dual recycling. When maximum response is sought, losses must be taken into account. In that case, with a compound cavity length much greater than the length of the SRC, the response for doubly resonant recycling is twice

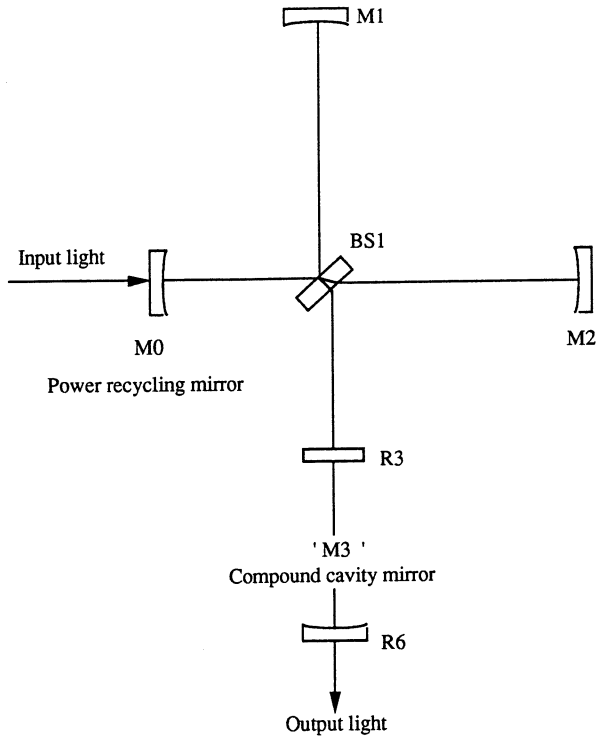

Fig. 6. Optical arrangement for compound doubly resonant signal recycling.

that of the equivalent dual recycling case at the expense of reduced response bandwidth; with equal length cavities, as could be more easily arranged in a real system, the bandwidth is the same with the gain in response reduced to a factor of $\sqrt{2}$. Provided $\omega_g \tau \ll 1$, where τ is the storage time of the light in the SRC, the optimum response frequency is related to the transmission T3 of the first mirror of the compound cavity mirror (M3, see Fig. 6) via $\omega_g = \mathrm{T3}/\sqrt{(\tau\tau')}$, where τ' is the light storage time in the compound cavity mirror. The bandwidth is mainly determined by the transmission of mirror M6.

Fig. 7 displays the frequency response of a doubly resonant system with equal reflectivity mirrors in the compound cavity mirror, for various reflectivity values (R3). The physical pathlengths of the SRC and the compound mirror are the same. As predicted, increasing τ' (increasing R3) reduces the frequency of optimum response. Comparison with Fig. 5 shows that for the R3 optimised for 4 kHz (R3 = 0·875) the doubly resonant case is about a factor of 2 more sensitive in comparison with tuned dual recycling, with the bandwidth reduced by the same factor, as predicted for this case where losses are not important.

(2f) Resonant Sideband Extraction (RSE)

Proposed by Mizuno *et al.* (1993), an interferometer can be operated in this mode when Fabry–Perot arm cavities are used. The configuration is identical to that for signal recycling, shown in Fig. 2. In Section 1 it was pointed out

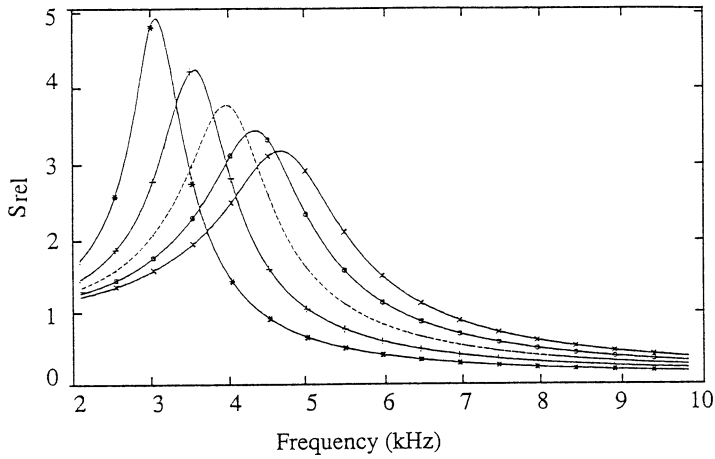

Fig. 7. Frequency response of a doubly resonant signal recycling interferometer relative to a power recycling interferometer. The compound cavity 'mirror' M3 has been chosen to be a symmetric cavity with reflectivity R3. The curves, in order of increasing peak response, correspond to R3 = 0·825, 0·85, 0·875 (dashed), 0·9 and 0·925, with corresponding frequency of optimum response given by 4·665, 4·335, 4·0 (dashed), 3·45 and 3·0 kHz. Other parameters are as for Fig. 5.

that signal frequencies can only be stored in the arm cavities for a time of the order of half the gravitational wave period. There is no such restriction on the carrier light. Now, from the view point of an observer outside mirror M3, the recycling configuration looks like two coupled cavities (see Fig. 8*a*). Mirror M3 with the inboard mirrors of the Fabry–Perot cavities (M4 or M5) acts like a frequency dependent mirror in a similar way to the cavity 'mirror' of the compound doubly resonant signal recycling configuration, described in Section 2*e*. By appropriate tuning of this cavity mirror, it can be made resonant with sideband light impinging on it from interferometer arms, but highly reflective for carrier light. Thus, the arm cavities can exhibit different storage times for carrier and signal: an extremely high finesse and therefore long carrier storage time; and optimum signal storage times.

From Fig. 8 it can be seen that compound signal recycling (with no Fabry–Perot arm cavities) and resonant sideband extraction are geometrically equivalent. Indeed resonant sideband extraction displays qualitatively similar frequency responses to those of the compound arrangement, shown in Fig. 7.

The major benefit of the resonant sideband arrangement is that the circulating power in the arm cavities can be made very large. This reduces the need for high power to pass through the main beamsplitter, the component most likely to exhibit thermal distortions. The more general question of the sensitivity of the various recycling arrangements discussed above to wavefront distortions will be pursued in the next section.

3. Distortions in Recycling

In an analysis based on Hermite–Gauss spatial modes, the fundamental mode propagating in an interferometer is the TEM00 mode. Various imperfections can

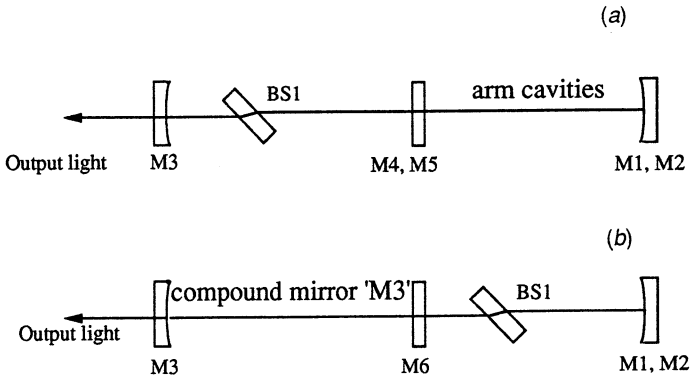

Fig. 8. (*a*) Equivalent three mirror configuration for resonant sideband extraction. The arm cavities are folded on top of each other, from the viewpoint of an observer looking through M3. (*b*) Equivalent three mirror configuration for doubly resonant signal recycling, without arm cavities.

scatter light from this mode into higher order spatial modes. For example, tilt on the end mirrors of a Michelson interferometer scatters light primarily into the TEM10, 01 modes; curvature mismatch scatters light into the cylindrically symmetric TEM02, 20 modes (Meers and Strain 1991; Vinet *et al.* 1992); thermal distortions in mirror substrates and coatings or beam splitters, apart from absorbing power, tend to scatter light primarily into TEM02, 20 modes (Winkler *et al.* 1991; Hello and Vinet 1993; Strain *et al.* 1994); some imperfections in mirror polishing/coating process have been shown to also scatter light into these modes (Schilling 1995). At the main beam splitter, the light in these higher order modes is directed toward the output along with the signal.

Interferometers with no recycling, or power recycling only, are very sensitive to distortions. Distorted light easily escapes the system via the beam splitter, and is absorbed in the photodetection system. This reduces the signal-to-noise ratio S/N in two ways: first, less power circulating in the power recycling cavity reduces the instrument's signal response; second, extra light on the photodetectors increases shot noise. This is in contrast to simple two mirror cavities. Simple cavities tend to be relatively tolerant to distortions because higher order modes must reflect off low transmission mirrors. There is therefore a tendency for such light to be trapped in the cavity, provided the distorted modes are non-resonant.

This situation is dramatically altered when tuned dual recycling is employed. Meers and Strain (1991) proposed that with the introduction of mirror M3 (see Fig. 2), much of the distorted light will be reflected back into the interferometer, with the reduction in transmission to the photodetection system being related to the transmittivity T3 of mirror M3 and the resonance condition of this light in the SRC. The reflected light can re-enter the PRC, contributing to the formation of a new normal mode for the system and maintaining the circulating power level.*

* In fact, if M3 was a 100% reflecting mirror, the PRC should then behave much like a simple cavity.

Such behaviour has been coined wavefront healing. Benchtop experiments performed by Meers and Strain (1991) support this scenario in the case of broadband dual recycling. McClelland *et al.* (1993) verified the predictions for delay line interferometers with various recycling arrangements, using numerical simulations. An example is shown in Fig. 9 for the case of curvature mismatch between the end mirrors of a one bounce delay line interferometer (Mavaddat *et al.* 1995). Even at (an unrealistically high) 10% mismatch, circulating power is only down by 10% for a modest signal recycling mirror reflectivity of 0·95. In comparison, without signal recycling, circulating power is down by 30%. At low distortions levels, power leakage can be reduced by more than a factor of 10 using dual recycling. Furthermore, McClelland *et al.* showed that the input mode couples effectively into the PRC, whilst the signal mode can be efficiently extracted. This translates directly into a much greater tolerance to wavefront distortions of tuned dual recycling interferometers compared to power recycling instruments (Fig. 10).

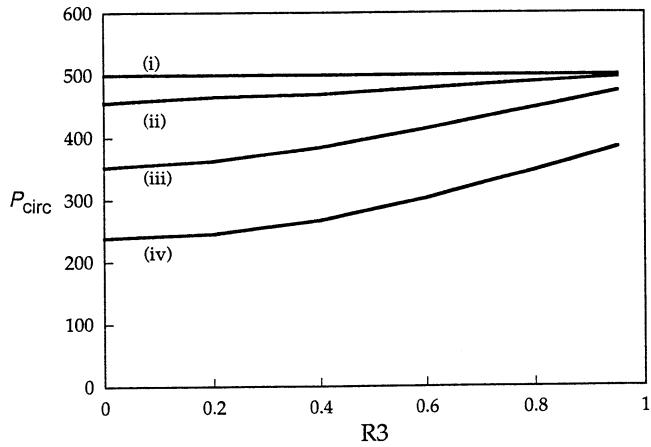

Fig. 9. Power circulating in the power recycling cavity versus R3, the amplitude reflectivity of the signal recycling mirror for (i) 0%, (ii) 5%, (iii) 10% and (iv) 15% curvature mismatch between mirrors M1 and M2. Pump power is 10 W, with a power recycling gain of 50 in the ideal case. Mirrors M0 and M3 are plane; mirrors M1 and M2 have curvature of 3450 m, at 0% mismatch. All mirrors have 1.e-04 intensity loss.

Broadband dual recycling interferometers, though significantly better than power recyclers, were found to be not as robust as the tuned case. This is because at high distortion levels, light is also scattered into the TEM00 mode. In broadband dual recycling, the SRC is tuned to the carrier, hence the TEM00 mode, and thus this distorted light is resonantly enhanced about the same factor as the signal. In addition R3 must be kept low to ensure that both sidebands remain approximately resonant.

With the introduction of the compound cavity mirror, even greater reduction in loss is observed since transmission through the output 'mirror' now depends on the the transmittivity of two mirrors and the resonance condition of the modes in

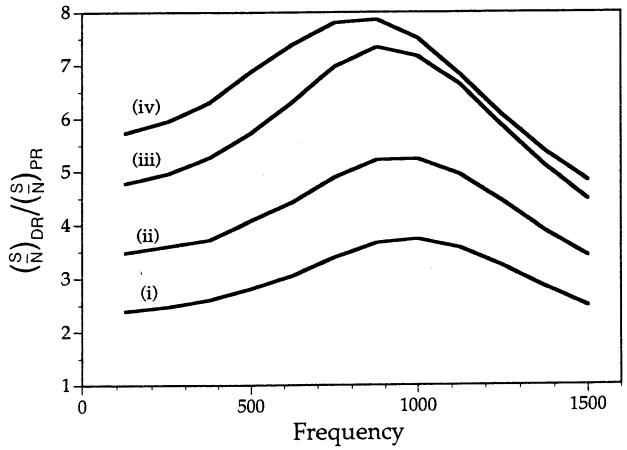

Fig. 10. Signal-to-noise ratio S/N of the dual recycling interferometer of Fig. 9, relative to the S/N of a power recycling interferometer, as a function of frequency, in the presence of different levels of curvature mismatch. Parameters and labels are as in Fig. 9.

both the SRC and the compound cavity. Numerical modelling shows a reduction in loss an order of magnitude better than for dual recycling (McClelland *et al.* 1993).

Though dual recycling delay line interferometers exhibit distortion tolerance, will devices with arm Fabry–Perot cavities be similarly tolerant? In the absence of signal recycling, the presence of wavefront distortion in one of the arm cavities reduces its finesse with light in higher order spatial modes being reflected toward the beam splitter, where it is ejected from the interferometer. The question to be addressed was whether dual recycling could maintain the power circulating in not only the power recycling cavities, but also in the arm cavities. Does the new 'normal mode' of the device couple effectively into both arm cavities? Preliminary results with a numerical simulation of a dual recycling interferometer with Fabry–Perot arm cavities (Stanley 1994; Stanley and McClelland 1995), see Fig. 11, indicates that this does indeed occur. At a tilt of 15% of the beam divergence applied to mirror M2 (see Fig. 2), with R3 set to 0·9, the power level in all cavities is still within 4% of the ideal. This is in contrast to power recycling only (R3 = 0·0), where power levels are down by almost 50%.

Resonant recycling when employed with power recycling also tends to force distorted light to remain in the system. This configuration should therefore show tolerance to distortions at a level similar to dual recycling. The advantage of dual recycling is its relative simplicity.

The final recycling arrangement discussed above was resonant sideband extraction (RSE). As noted earlier, the configuration is identical to dual recycling with Fabry–Perot arm cavities, the difference arising from the chosen resonance conditions of the coupled cavities. The major advantage of RSE lies in the capacity to store large amounts of optical power in the interferometer arms (Mizuno *et al.* 1993). This alleviates the need for an high finesse PRC, significantly reducing thermal loading on the main beam splitter. Mizuno *et al.* saw this arrangement

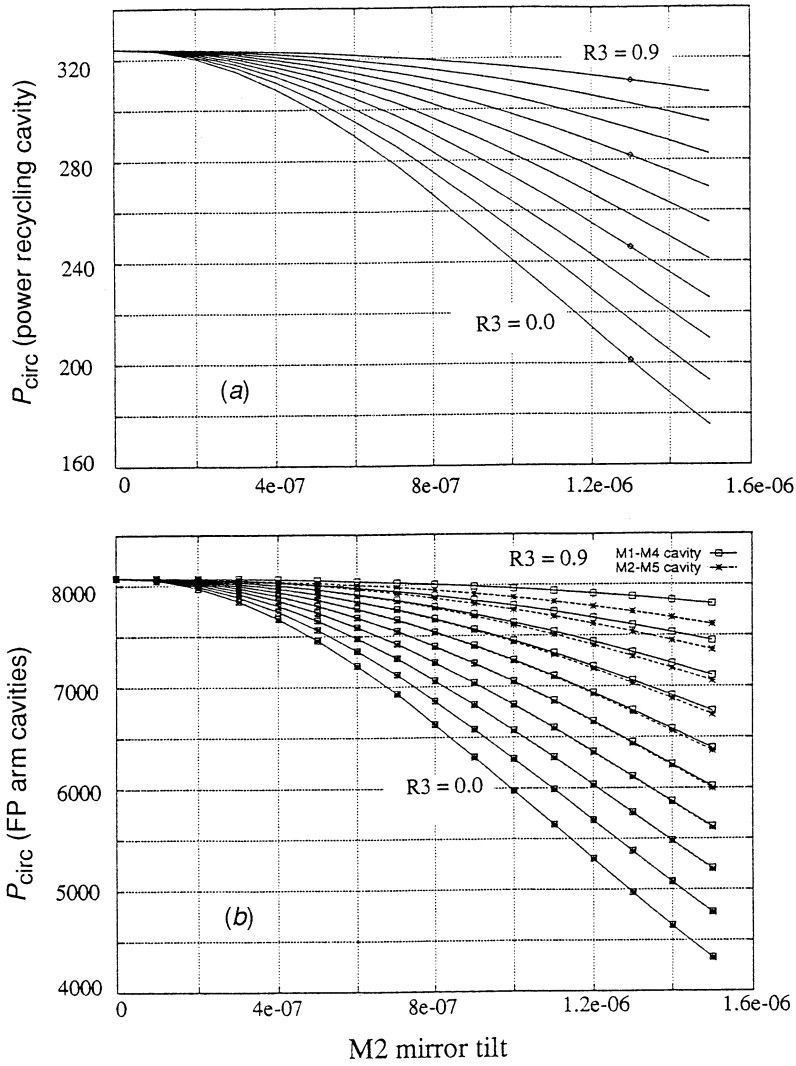

Fig. 11. (*a*) Power build-up in the power recycling cavity in a dual recycling interferometer, with arm Fabry–Perot cavities, as a function of tilt of mirror M2 (see Fig. 2). (*b*) Power build-up in the arm cavities, labelled in Fig. 2, as a function of the tilt of M2. R3 is varied from 0 to 0·9, while R0 and R4 (R5) are held fixed at 0·95 and 0·9608 respectively. Circulating power at no distortion is in agreement with the analytic solution. The tilt is in radians. All mirrors are curved and the beam divergence in the arm cavities is 9·9e-06 rad. Input laser power is 10 W. For full details see Stanley *et al.* (1995).

as the most likely way to build an effective broadband recycling interferometer. However, low PRC finesse means low power recycling mirror reflectivity, R0. This may then permit light scattered into higher order modes by imperfections, to again leak from the interferometer, reducing the response. This could be

compensated for by increasing R0. It is therefore likely that there is an optimum set of mirror reflectivities which keep thermal loading tolerably low but enable wavefront healing to be effective. Investigation into this question is in progress.

4. Application of Recycling to 'Real' Interferometers

The techniques discussed in Section 2 are applicable to interferometers which are limited by photon noise. As described in the Introduction, and summarised in Fig. 1, gravitational wave detectors are afflicted by other serious noise problems, the most of important of which is thermal noise. Given this, and considering that predicted sources of gravitational waves usually lie below 2 kHz, the usefulness of these techniques in mid to long baseline instruments will now be examined.

Long baseline interferometers currently under construction will have baselines of either 3 (VIRGO) or 4 (LIGO) km. Pumped by around 10 W of laser power and with power recycling factors of around 20, these instruments will be seismic and thermal noise dominated up to a few hundreds of kiloHertz, and not truly photon noise limited until 2 kHz. Nevertheless, Fig. 1(ii) is a plot of a possible frequency sensitivity for a 3 km instrument, based on VIRGO parameters, with signal recycling included (Mavaddat *et al.* 1995). The signal recycling mirror has been tuned to 1 kHz, with an amplitude reflectivity of 0·8 chosen to maintain the interferometer bandwidth out to 2 kHz. At 1 kHz, the sensitivity is improved by a modest factor of 1·3. The significance however lies in the tolerance to wavefront distortions this instrument will now have. Perhaps this could 'return' an imperfect device to its design specification.

Recently, there have been a number of proposals to build mid-baseline (400 to 600 m), advanced technology interferometers (Hough *et al.* 1994; Sandeman *et al.* 1995). As proposed these instruments employ state-of-the art optical technology in three bounce delay dual recycling interferometers. Power recycling factors of the order of 1700 with signal recycling factors of the order of 800 are suggested. This represents 7 to 14 kW of laser power (5 to 10 W of input power) on the beam splitter. They are designed with the tolerance benefits of dual recycling in mind.

Figs 12 and 13 summarise the predictions for AIGO 400, the Australian project. Shown in Fig. 12 are shot noise curves for four different recycling factors. Curves (*a*) and (*c*) are based on application of recycling factors already achieved in the laboratory; curves (*b*) and (*d*) employ the goal factors. Fig. 13 plots the predicted sensitivity, including seismic, thermal and shot noise for the first (curve *a*) and goal (curve *b*) stages of AIGO 400. The goal thermal noise floor (curve *c*) is based on predictions from suspension system results already achieved at the University of Western Australia. This instrument is photon noise limited above 30 Hz. It should be capable of approaching the sensitivity levels of stage 1 long baseline instruments over a bandwidth of a few hundred Hertz. Given even further progress in mirror technology it should be possible to 'dig holes' in this noise spectrum, down to the thermal noise limit (curve *c* in Fig. 13) at selected frequencies, using highly narrowbanded signal recycling. For example, with total SRC power loss of around 50 ppm the thermal noise floor in Fig. 13 could be reached at 1 kHz over a bandwidth of about 50 mHz. This type of performance suggests that such instruments could play an important and exciting role in gravitational wave detection before the end of this decade.

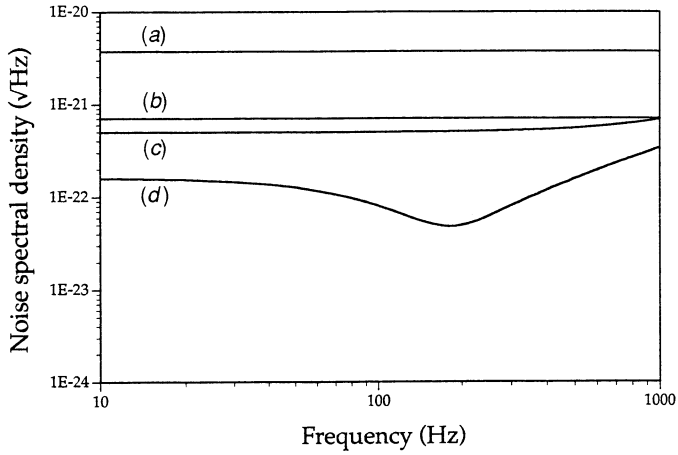

Fig. 12. Predicted photon noise limited noise spectral density versus frequency for AIGO 400, with input power 5 W. Curve (*a*), power recycling factor of 60, no signal recycling; (*b*) power recycling factor of 1700; (*c*) dual recycling with power and signal recycling factors of 60; and (*d*) power recycling factor of 1700 and signal recycling factor of 800.

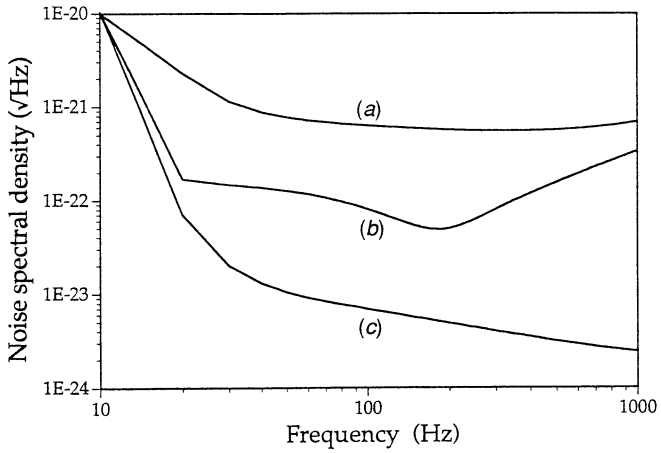

Fig. 13. Predicted noise spectral density as a function of frequency for AIGO 400: (*a*) first stage parameters; (*b*) goal parameters (refer to Fig. 12); and (*c*) goal thermal plus seismic noise limit. With improvements in mirror technology, dual recycling instruments could reach this noise floor at a tuned frequency over a very narrow bandwidth.

5. Conclusions

In this paper an overview of techniques known collectively as recycling has been presented. The first of these methods, power recycling, has already been factored into the performance of long baseline laser interferometer gravitational wave detectors presently under construction. Many of the configurations turn

an inherently broadband instrument into a resonant detector, enhancing the sensitivity over a narrower bandwidth. These systems tend to display much greater tolerance to wavefront distortions than the power recycling configuration.

Of the resonant techniques, dual recycling is perhaps the simplest to implement. Mid-baseline interferometers employing three bounce delay line arms and dual recycling have recently been proposed. These instruments should be capable of reaching the sensitivity of the first generation of long baseline interferometers, over a restricted bandwidth. When operated in coincidence with long baseline detectors they may well have observational capability. Potential developments in suspension system and mirror technology open the possibility of making an ultra-narrowband instrument of high sensitivity, tunable to predicted sources.

Currently the best configuration for a broadband detector is resonant sideband extraction. The ability to store large amounts of power in the interferometer arms will avoid many problems associated with thermal distortion of the main beam splitter. Optimum choice of mirror reflectivities should ensure effective wavefront healing. However, the many and varied recycling proposals generated over the last ten years suggest that there is yet more to come.

Acknowledgments

The author would like to thank R. Mavaddat, P. Hello, J.-Y. Vinet and B. D. Stanley for their contributions to the numerical simulation research.

References

Bondi, H. (1957). *Nature* **179**, 1072.

Brillet, A., Jacquemet, M., Giazotto, A., *et al.* (1992). VIRGO Final Conceptual Design, unpublished.

Caves, C. M. (1980). *Phys. Rev. Lett.* **45**, 75–8.

Caves, C. M. (1981). *Phys. Rev.* D **23**, 1693–1708.

Del Fabbro, R., di Virgilio, A., Giazotto, A., Kautzky, H., Montelatici, V., and Passuello, D. (1988). *Phys. Lett.* A **132**, 237.

Drever, R. W. P. (1983). *In* 'Gravitational Radiation' (Eds N. Deruelle and T. Piran), p. 321 (North Holland: Amsterdam).

Einstein, A. (1915*a*). 'Zür allgemeinen Relativitätstheorie', *Preuss. Akad. Wiss. Berlin Sitzber*, pp. 778–86 (Nov. 11).

Einstein, A. (1915*b*). 'Zür allgemeinen Relativitätstheorie (Nachtrag)', *Preuss. Akad. Wiss. Berlin Sitzber*, pp. 799–801 (Nov. 18).

Einstein, A. (1915*c*). 'Erklärung der Perihelbewegung des Merjur aus der allgemeinen Relativitätstheorie (Nachtrag)', *Preuss. Akad. Wiss. Berlin Sitzber*, **47**, 831–9 (Nov. 25).

Einstein, A. (1915*d*). 'Die Feldgleichungen der Gravitation', *Preuss. Akad. Wiss. Berlin Sitzber*, pp 844–7 (Dec. 2).

Einstein, A. (1916). Sitzungsberichte der physikalischmathematischen Klasse. *Preuss. Akad. Wiss. Berlin* p. 154.

Fritschel, P., Shoemaker, D., and Weiss, R. (1992). *Appl. Opt.* **31**, 1412.

Gersenshtein, M. E., and Pustovoit, V. I. (1963). *Sov. Phys. JETP* **16**, 433.

Gray, M. B. (1995). Quantum noise limited interferometry. PhD thesis, Australian National University, unpublished.

Hamilton, W. (1995). Proc. 7th Marcel Grossman Meeting on General Relativity (World Scientific: Singapore) (in press).

Hello, P., and Vinet, J.-Y. (1993). *Phys. Lett.* A **178**, 351.

Hough, J., Danzmann, K., Schutz, B. F., Bennett, J.R.J., Kose, V., *et al.* (1994). GEO 600: Proposal for a 600 m Laser-Interferometric Gravitational Wave Antenna, unpublished.

Ju, L., and Blair, D. G. (1994). *Meas. Sci. Technol.* **5**, 1053.

McClelland, D. E., Savage, C. M., Tridgell, A. J., and Mavaddat, R. (1993). *Phys. Rev.* D **48**, 5475.

Maischberger, K., Rüdiger, A., Schilling, R., Schnupp, L., Winkler, W., and Leuchs, G. (1988). *In* 'Experimental Gravitational Physics' (Eds P. F. Michelson *et al.*), p. 316 (World Scientific: Singapore).

Man, C. N., Shoemaker, D., Pham Tu, M., and Dewey, D. (1990). *Phys. Lett.* A **148**, 8.

Mavaddat, R., McClelland, D. E., Hello, P., and Vinet, J.-Y. (1995). Dual recycling laser interferometer gravitational wave detectors: simulating the performance with imperfect mirrors, *J. Opt.* (in press).

Meers, B. J. (1988). *Phys. Rev.* D **38**, 2317.

Meers, B. J., and Drever, R. W. P. (1992). Doubly-resonant signal recycling for interferometric gravitational wave detectors, preprint, University of Glasgow.

Meers, B. J., and Strain, K. A. (1991). *Phys. Rev.* D **43**, 3117.

Mizuno, J., Strain, K. A., Nelson, P. G., Chen, J. M., Schilling, R., Rüdiger, A., Winkler, W., and Danzmann, K. (1993). *Phys. Lett.* A **175**, 273.

Moss, G. E., Miller, L. R., and Forward, R. L. (1971). *Appl. Opt.* **10**, 2495.

Pirani, F. A. E. (1957). *Phys. Rev.* **105**, 1089.

Raab, F. J. (1995). Proc. First Edoardo Amaldi Conference on Gravitational Wave Experiments, LIGO Preprint, pp. 94–9.

Regehr, M. (1994). Signal extraction and control for an interferometric gravitational wave detector, PhD thesis, Caltech, unpublished.

Sandeman, R. J., Blair, D. G., McClelland, D. E., Munch, J., Walsh, C., Lun, A., Bishop, A., Capizzi, V., and Incoll, R. (1995). Australian International Gravitational Wave Observatory (Phase 1) (AIGO 400), unpublished.

Saulson, P. R. (1990). *Phys. Rev.* D **42**, 2437.

Saulson, P. R. (1991). *In* 'Gravitational Astronomy: Instrument Design and Astrophysical Prospects' (Eds D. E. McClelland and H.-A. Bachor), p. 248 (World Scientific: Singapore).

Schilling, R. (1995). Proc. 7th Marcel Grossman Meeting on General Relativity (World Scientific: Singapore) (in press).

Stanley, B. D. (1994). Numerical modelling of an interferometric gravitational wave antenna, Honours Thesis, Australian National University, unpublished.

Stanley, B. D., and McClelland, D. E. (1995). Wavefront healing in Fabry–Perot Michelson interferometric detectors of gravitational waves, preprint, Australian National University.

Stevenson, A. J., Gray, M. B., Harb. C. C., McClelland, D. E., and Bachor, H.-A. (1995). *Aust. J. Phys.* **48**, 971.

Strain, K. A., and Meers, B. J. (1991). *Phys. Rev. Lett.* **66**, 1391.

Strain, K. A., Danzmann, K., Mizuno, J., Nelson, P. G., Rüdiger, A., Schilling, R., and Winkler, W. (1994). *Phy. Lett.* A **194**, 124.

Tobar, M. E., Blair, D. G., Ivanov, N. E., van Kann, F., Linthorne, N. P., Turner, P. J., and Heng, I. S. (1995). *Aust. J. Phys.* **48**, 1007.

Tsubono, K. (1995). Proc. 7th Marcel Grossman Meeting on General Relativity (World Scientific: Singapore) (in press).

Vinet, J.-Y., Hello, P., Man, C. N., and Brillet, A. (1992). *J. Phys. (Paris)* **2**, 1287.

Vinet, J.-Y., Meers, B. J., Man, C. N., and Brillet, A. (1988). *Phys. Rev.* D **38**, 433.

Vogt, R. (1991). Proc. 6th Marcel Grossman Meeting on General Relativity (Eds H. Sato and T. Nakamura), p. 244 (World Scientific: Singapore).

Ward, H., Hough, J., Killbourn, S., Morrison, E., Newton, G. P., Robertson, D. I., Robertson, N. A., Skeldon, K., and Strain, K. A. (1995). Proc. 7th Marcel Grossman Meeting on General Relativity (World Scientific: Singapore) (in press).

Weber, J. (1966). *Phys. Rev.* **146**, 935.

Weber, J. (1987). Proc. Sir Arthur Eddington Centenary Symposium, Vol. 3 (Eds J. Weber and T. M. Karade), p. 1 (World Scientific: Singapore).

Winkler, W., Danzmann, K., Rüdiger, A., and Schilling, R. (1991). *Phys. Rev.* A **44**, 7022.

Manuscript received 20 February, accepted 6 June 1995